BULLETIN OF THE POLISH ACADEMY OF SCIENCES
TECHNICAL SCIENCES, Vol. 71(2), 2023, Article number: e144618
DOI: 10.24425/bpasts.2023.144618

Study of Si morphology in AlSi21CuNiMg cast alloy using colour and deep etching

Eva TILLOVÁ [1]*, Mária CHALUPOVÁ [1], Lenka KUCHARIKOVÁ [1], Mirosław BONEK [2], Milan UHRÍČIK [1], and Lucia PASTIEROVIČOVÁ [1]

[1] University of Žilina, Faculty of Mechanical Engineering, Department of Materials Engineering, Univerzitná 8215/1, 010 26 Žilina, Slovak Republic
[2] Silesian University of Technology, Faculty of Mechanical Engineering, Department of Engineering Materials and Biomaterials, ul. Konarskiego 18A, 44-100 Gliwice, Poland

Abstract. The effect of possible modification and refining effect of Al–Cu–P-based pre-alloy combined with Fe on the microstructure and the silicon morphology change in hypereutectic Al–Si cast alloy was studied. The samples in the as-cast state were observed by optical and scanning electron microscopy with energy-dispersive X-ray spectroscopy. The 3D morphology of both primary and eutectic silicon was observed by using colour and deep etching in detail. The results showed that the AlCu19P1.4 pre-alloy (1.07 wt.%) combined with the addition of Fe (0.02 wt.%) has a significant effect on the change of the amount, size and morphology of primary Si. This is significantly refined and changes the shape from a coarse irregular star-shaped, polyhedral, or plate-like shape to a fine polyhedral shape. The average size of the primary Si is reduced by about of 78% from 135 μm to 28 μm and the number of primary Si particles increased from 7.4 to 237. No change in the morphology of the eutectic Si was observed; a refinement of the structure from a coarse needle/plate-like to a fine plate-like structure was seen. The depth etching method using HCl was very effective in the study of the 3D silicon morphology observed, which could be observed in detail without the presence of artefacts.

Key words: Al–Si cast alloy; primary silicon; deep etching; morphology.

1. INTRODUCTION

Al-alloys with Si content higher than 13% belong to the so-called hypereutectic alloys. Conventional alloys usually have more than 14% Si and more recently alloys with about 18-20% Si or more have been used. Other elements in hypereutectic Al–Si alloys are Cu, Mg, Mn, and Ni. The share of hypereutectic Al–Si alloys in the total volume of Al–Si alloys is relatively low. These alloys were first used more than 50 years ago, primarily for the casting of pistons for engines and are already used for this application today [1], in the aerospace, shipbuilding and automotive industries. Hypereutectic Al–Si alloys are currently receiving increasing attention due to their excellent properties compared to hypoeutectic and eutectic Al–Si alloys, in response to the much more demanding requirements placed on materials for automotive engines (engine blocks, pistons, valve retainers, compressors, pumps, cylinders and cylinder liners, which are good alternatives to cast iron, which can significantly reduce the weight of automobiles) [1, 2].

The main reason for their use is the high hardness of the primary silicon, which gives these alloys a high wear resistance and a thermal expansion coefficient about 15% lower than that of hypoeutectic alloys. The alloys have generally good mechanical properties, but the toughness is low. There are also characterized by high corrosion resistance, excellent castability, low specific gravity, and good thermal conductivity. The wear resistance of these alloys is achieved by a higher silicon content, which also increases their strength. However, the improvement in strength and wear resistance is at the expense of machinability and castability [3, 4].

A progressive material is the alloy AlSi21CuNiMg. Compared to other hypereutectic alloys it is characterized by high mechanical properties, low thermal expansion and high thermal conductivity. These properties are especially important in thin-walled castings for modern engines with a high specific power.

The microstructure of alloys with Si content of more than 13% consists of eutectic (eutectic Si particles in the Al-matrix) and primary Si. The crystallization of hypereutectic Al–Si alloys begins with the formation of primary silicon. The nucleation nuclei are exclusively aluminium phosphide particles AlP. Due to the common phosphorus content of only a few ppm, there is a relative lack of suitable crystallization nuclei. Therefore, the initiation of crystallization occurs at significant supercooling below the equilibrium liquidus temperature of up to several degree Celsius.

The small number of active nuclei results in the formation of large Si-crystals. Depending on the solidification conditions, in traditional casting processes, the primary silicon particles are star-shaped (5 axes emanating from one nucleus – star-like), a plate (plate-like), a polyhedral (hexagonal or octagonal), or dendritic. Different shapes can also occur in a structure.

*e-mail: eva.tillova@fstroj.uniza.sk

Manuscript submitted 2022-10-11, revised 2022-11-22, initially accepted for publication 2022-12-27, published in April 2023.

Although the large hard silicon particles give the alloy excellent wear resistance, they also make machinability difficult. Solidification is completed by the crystallization of the eutectic. Eutectic Si in these alloys is present as a thick needle, which can lead to earlier crack initiation and tensile fracture and deterioration of mechanical properties [3, 5, 6]. Therefore, refinement of primary Si and modification of eutectic Si are the key to improving mechanical properties.

In praxis, it is difficult to refine primary Si and at the same time modify eutectic Si by standard chemical refinement methods. For this reason, research studies have been conducted on modifiers and refiners, such as Na, Sr, Sb, P, La, Nd, Bi, Y [3, 7–15], semi-solid processing [16, 17], electromagnetic stirring [18], magnetic field [19], quench modification [2], etc. Among all the previously referred methods, the addition of modifiers or refiners to the hypereutectic Al–Si alloy is still the most widely used in the industry due to its simplicity and efficiency.

Phosphorus is an effective refiner of primary Si. It reacts with the liquid aluminium to form large numbers of aluminium phosphide (AlP) nuclei on which much smaller primary silicon particles crystallize than in the unrefined alloy. Today, the most common refinement is achieved by adding about 30–60 ppm of phosphorus in the form of Al–P, Al–Cu–P, Al–Fe–P, Al–Zr–P, Cu–P, and Cu–Fe–P (for alloys that contain Cu), Fe–P and Ni–P [21–24].

The particle size of the primary silicon is by phosphorus refinement reduced to 10–30 µm. The higher the silicon content of the alloy, the higher the phosphorus dosage must be. The refinement of the structure is reflected in improved machinability and increased mechanical properties. The abrasion resistance is unchanged. Researchers [25, 26] found that the effect of the refinement of the primary Si-crystals could be activated with an iron micro additive that can form FeP-phase particles. As for refining or modifying eutectic Si, however, phosphorus is ineffective.

Many researchers are focusing on improving modifiers to meet the requirements of environmental protection and industrial applications. In the present study, a novel refinement process combining Al–Cu–P and Fe-micro additive is investigated to modify/refine primary Si in a hypereutectic AlSi21CuNiMg alloy. The change of 2-D and 3-D morphology of primary Si by colour and depth etching was observed.

2. MATERIALS AND METHODS

AlSi21CuNiMg cast alloy (KS 280) was used as the experimental material. This alloy belongs to the group of hypereutectic Al–Si alloys [11, 27, 28] and is suitable for pistons for high-performance combustion engines. The experimental alloy was melted in an electric resistance furnace. The whole melting was carried out at a temperature of 810–840°C. The alloy was poured into the metallic moulds heated to a temperature of 200–300°C. The refining process was carried out using hexachloroethane at 0.15% by weight of the charge. After removing the slag from the metal level, modification treatments were carried out.

Three experimental melts were obtained (marked as alloy A, alloy B and alloy C). The chemical composition of the experimental alloy (tolerance limits) is given in Table 1 and the composition of the melts in Table 2. Test bars (diameter 20 mm, length 300 mm) were cast.

Table 2
Experimental alloys

Alloy	
A	–
B	1.07% AlCu19P1.4
C	1.07% AlCu19P1.4 + 0.02% Fe

The chemical analysis of the experimental cast AlSi21CuNiMg alloy was carried out by arc spark spectroscopy (SPECTROMAX spectrometry). Alloy A was not modified. Alloys B and C were refined by phosphorus. Phosphorus was added in the form of AlCu19P1.4 pre-alloy. This pre-alloy (Al–Cu–P) is a high-performance grain refiner specially developed to produce the highly demanding hypereutectic Al–Si alloys. Refining of alloy B was carried out by adding 1.07% AlCu19P1.4. Alloy C has also been refined by the addition of AlCu19P1.4 pre-alloy with an iron micro additive (0.02% Fe) used in powdered form.

The microstructure of the experimental alloys was analyzed using a Neophot 32 optical microscope (OM) and a VEGA LMU II scanning electron microscope (SEM) with energy-dispersive X-ray spectroscopy (Brucker Quantax EDX analyzer). The experimental samples were taken from the cast test bars by cutting with a Micron 3000 automatic saw with cooling to prevent microstructure deformation or heat generation. After cutting, samples for microscopic analysis were prepared by standard metallographic procedures (hot preparation in Bakelite, wet grinding on SiC papers, DP polishing with 3 µm diamond pastes and finally polishing with STRUERS OP-U commercial fine silica slurry).

The prepared samples were etched using Weck-Al etchant (100 ml H_2O, 1 g NaOH, 4 g $KMnO_4$). The Weck-Al etchant is used to increase the colour contrast in Al–Si alloys. The etchant is always prepared fresh. With this etchant, the etching time

Table 1
Chemical composition of the experimental AlSi21CuNiMg alloy (wt.%) and the composition limits

	Si	Cu	Mg	Mn	Ni	Fe	Zn	Ti	Al
Standard (KS 280) [28]	20–22	1.4–1.8	0.4–0.6	0.4–0.6	1.4–1.6	max. 0.7	max. 0.2	max. 0.2	Bal.
Experimental alloy	21.2	1.5	0.58	0.45	1.52	0.45	0.2	0.05	Bal.

is difficult to choose (5 to 45 seconds is recommended) and must always be determined experimentally depending on the chemical composition of the experimental alloy.

The samples must be completely immersed in the solution. During the etching, a turbulent reaction of the sample surface with the etchant can be observed. The degree of etching is checked optically, the surface of the sample is etched if it shows a brown-blue-coloured surface. After etching with Weck-Al etchant, the Si is usually coloured dark brown or dark blue and the intermetallic phases stay light.

After the preliminary evaluation and documentation of samples on an optical and electron microscope, the samples were deep etched. The deep etching aims to dissolve the aluminium matrix and reveal the three-dimensional morphology of the Si or intermetallic phases. The deep etching was carried out for 30 s in HCl solution (36 ml HCl, 100 ml distilled water) in a laboratory glass dish at ambient temperature. The samples were held by hand so that it is immersed in the etchant with the surface to be evaluated facing downwards and the samples were lightly moved to prevent etching products from sedimenting on the surface of the sample.

The deep etching time for Al–Si alloys was experimentally determined to be between 30 s and 2 min. Etching times of less than 30 s are usually insufficient to reveal the Si morphology. Exceeding the etching time of 2 min has no practical relevance because no new knowledge of Si-morphology will be obtained by further etching. The etching time was controlled optically. The sample is considered to be etched after the so-called surface darkening. Preliminary sample preparation before etching was usually not necessary, but the reduction of the surface deformed or contaminated layer can shorten the etching process [29]. Using the deep etching prepared samples, a three-dimensional Si-morphology was observed once it was scanned by the VEGA LMU II electron microscope.

Quantitative analysis of the primary Si was performed using a NEOPHOT 32 light microscope with a computer equipped with NIS Element 4.0 image analyzer software [30] to quantify the average size and quantity of the primary Si particles. To minimize the statistical errors in determination, 15 to 20 microphotographs were evaluated; a relative error of less than 0.05 was looked for.

3. RESULTS

The microstructures of the experimental alloys A, B and C after colour etching using Weck-Al etchant are documented in Fig. 1. Microstructure of the experimental alloy consists of primary silicon particles embedded in a binary eutectic matrix (α-aluminium dendrites + eutectic silicon). It is generally dependent on the rate of nucleation and cooling during solidification. As can be seen from Fig. 1, the number of primary Si particles per unit area increases as its size decreases due to the addition of phosphorus (Fig. 1, Table 3).

In the unmodified alloy A, there are coarse star-shaped and polyhedral primary Si particles and plate-like (in the plane of metallographic cut needle-like) eutectic Si in α-matrix (Fig. 1a). A great star-shaped and polyhedral primary Si shape predominate.

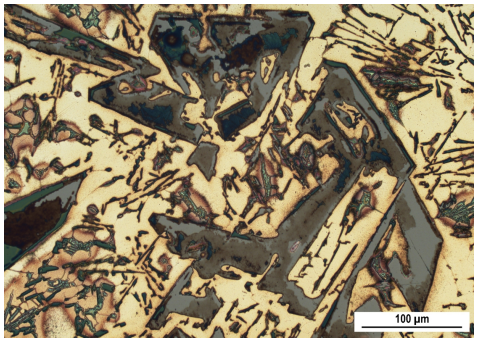

alloy A (without AlCu19P1.4)

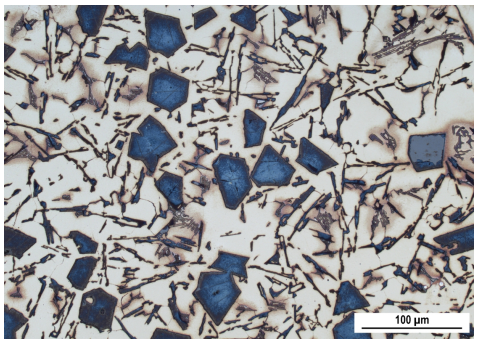

alloy B (1.07% AlCu19P1.4)

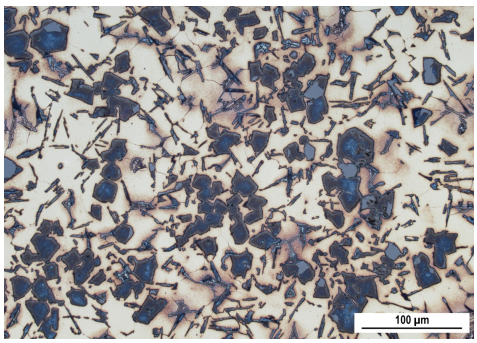

alloy C (1.07% AlCu19P1.4 + 0.02% Fe)

Fig. 1. Effect of AlCu19P1.4 and micro additive Fe on the microstructure (primary Si and eutectic structure) of AlSi21CuNiMg cast alloy, etch. Weck-Al

After refinement with Al–Cu–P, the primary Si was refined gradually (Fig. 1b and Fig. 1c), but eutectic silicon remains needle-like. In alloys B and C, which are modified by AlCuP (alloy B) and AlCuP + Fe-micro additive (alloy C), respectively, the star-shaped primary Si was not observed, only polyhedral or plate-like. Polyhedral morphology has a different

Table 3
Results of quantitative analyses

Alloy	The average size of primary Si (µm)	Number of primary Si particles
A	135 ± 54	7.4 ± 3
B	35.5 ± 0.73	115 ± 3
C	27.7 ± 3.14	237 ± 48

shape, depending on the orientation and sectioning of the polyhedron after polishing the metallographic cut (triangle, square, trapezoid, or hexagon – Fig. 1b and 1c).

Table 3 documented the result of the quantitative analysis of the primary Si particles. As the results of the quantitative analysis show, the average primary Si size was reduced by 78% from 135 μm (in alloy A) to 27.7 μm (in alloy C). On the other hand, the number of primary Si particles increased from an average of 7.4 (in alloy A) to 237 particles (in alloy C).

The SEM micrographs representing typical 3-D morphologies of primary Si in experimental alloys after deep etching by HCl are documented in Fig. 2. For the deep etching, we usually cannot use conventional etchants used for the light metallographic microscopy because these etchants have a low depth of attack and do not etch deep enough into the aluminium matrix.

Three types of primary Si were observed in Fig. 2: star-like or star-shaped (Fig. 2a); polyhedral (Fig. 2b) and plate-like (Fig. 2c). Fivefold star-shaped Si crystals can be observed usually in slowly cooled hypereutectic Al–Si castings and unmodified alloys. Figure 2a documents the typical star-shaped microstructure of primary Si crystals. It is observed that the star-shaped Si morphologies grow from decahedral nuclei. This nucleus consists of five Si-tetrahedrons in a twin orientation and shares a common ⟨110⟩ axis.

In agreement with the authors' work in [31–33], the Si-crystal growth through the branches can be explained by the TPRE (twin plane re-entrant edge) mechanism. The TPRE mechanism was first presented by Hamilton and Seindesticker [34] as an explanation for the growth of germanium dendrites and was later applied to Si-crystal growth. According to them, Si crystallizes continuously under equilibrium conditions with preferential growth in the planes ⟨111⟩.

Polyhedral or octahedral primary Si (Fig. 2b) occurs in a wide variety of shapes such as triangular, square, trapezoidal, and hexagonal random shapes because of random cutting induced during sample preparation (polishing). In the early stage of growth, the polyhedral primary Si nucleates to form a spherical or round shape.

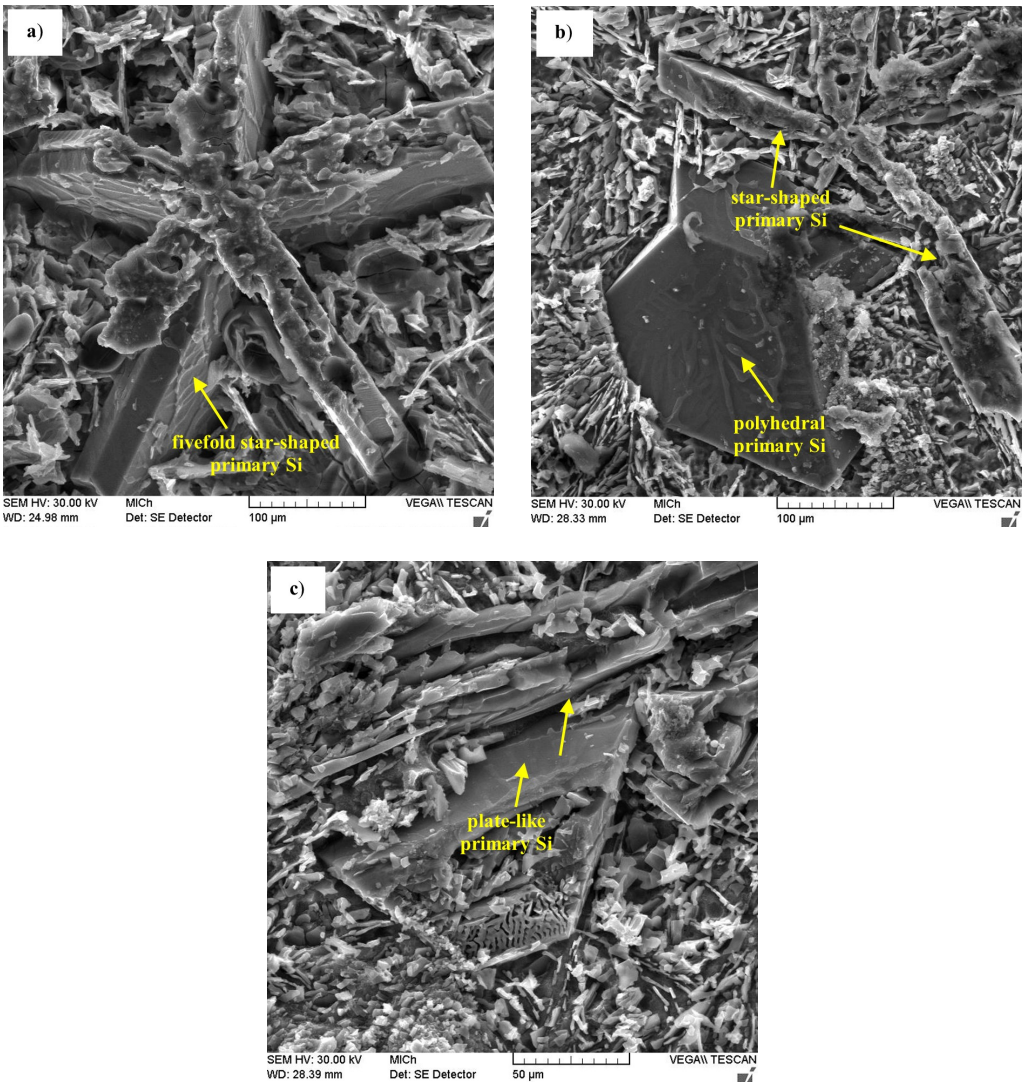

Fig. 2. Different shapes of primary silicon observed in experimental AlSi21CuNiMg cast alloy without AlCu19P1.4: a) star-shaped, b) polyhedral, c) plate-like; deep-etched by HCl, SEM

As the primary Si continues to gradually grow to larger sizes, above a critical size it would become unstable and expands, preferentially at the edges and vertices of the growing octahedral. Inside the Si-crystal, there are many so-called twinning planes. The twinning planes are planes that are always identical to some existing plane on the crystal, which can be described by Miller indices. A twinning plane usually has simple (low) Miller indices.

Generally, twinning is manifested by the formation of hollow angles greater than 180°, i.e. planes forming an exterior angle of 141°(the edges of the octahedron) or 219°(the vertex of the octahedron). The Si crystal is formed by gradual expansion from these twinning planes into the chamfered edges ⟨111⟩ and is drawn mainly in the ⟨112⟩ direction. At least two parallel planes are required for crystal growth to continue.

Silicon with flat-plate-like morphology (Fig. 2c) is commonly observed in unmodified Al–Si alloy. The hexagonal plate grows along the ⟨112⟩ direction by the TPRE growth mechanism. The Si-crystals grow anisotropically along the less tightly aligned planes until the crystal is lined only by the edges ⟨111⟩ [31–33].

The effect of the addition of AlCu14P1.4 (alloy B) and AlCu14P1.4 with Fe micro-addition (alloy C) on the morphology of primary Si in the experimental AlSi21CuNiMg alloy is documented in Fig. 3. The change in the morphology of primary Si can be as follows. A known method of Si growth after modification involves suppression of growth by the TPRE mechanism and the impurity-induced twin (IIT) mechanism. The TPRE mechanism of suppression assumes that the modifier atoms restrict the growth of the Si phase by selectively adsorbing onto the TPRE, thereby removing the growth advantages of Si on the TPRE.

The IIT mechanism suggests that the modifier atoms can adsorb on the growing planes ⟨111⟩ Si, thereby forming frequent multiple Si twins. It should be noted that either the suppression of the TPRE mechanism or the ITT mechanism may be related to the adsorption of modifier atoms in the Si phase [35].

As is seen in Fig. 3, AlCu14P1.4 master appears not only as a modifier but also as a refiner. Phosphorus reacts with liquid aluminium to produce probably a fine dispersion of heterogeneous AlP nucleant for primary Si which has a crystal structure like that of Si.

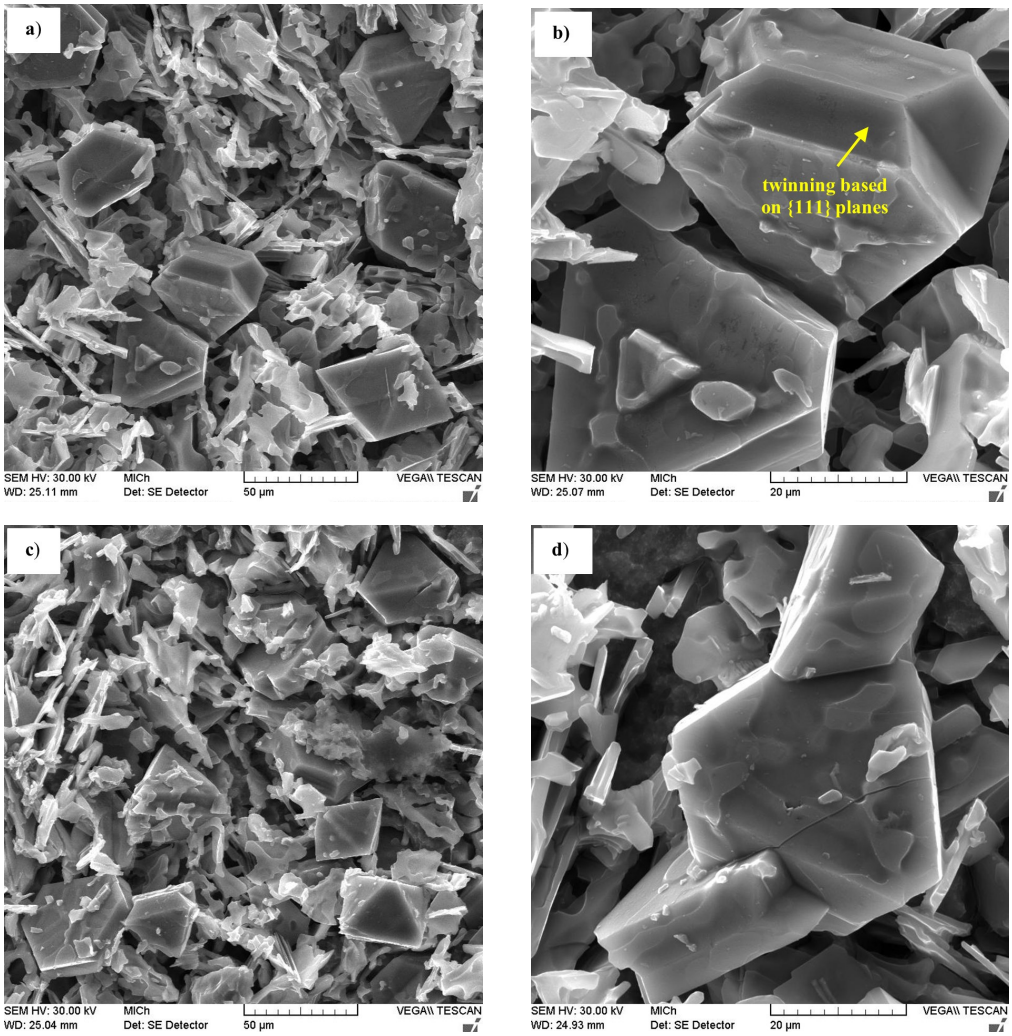

Fig. 3. 3-D morphology of primary Si in experimental AlSi21CuNiMg cast alloys: a) Si-distribution in alloy B, b) detail of Si-morphology in alloy B, c) Si-distribution in alloy C, d) detail of Si-morphology in alloy C; deep-etched by HCl, SEM

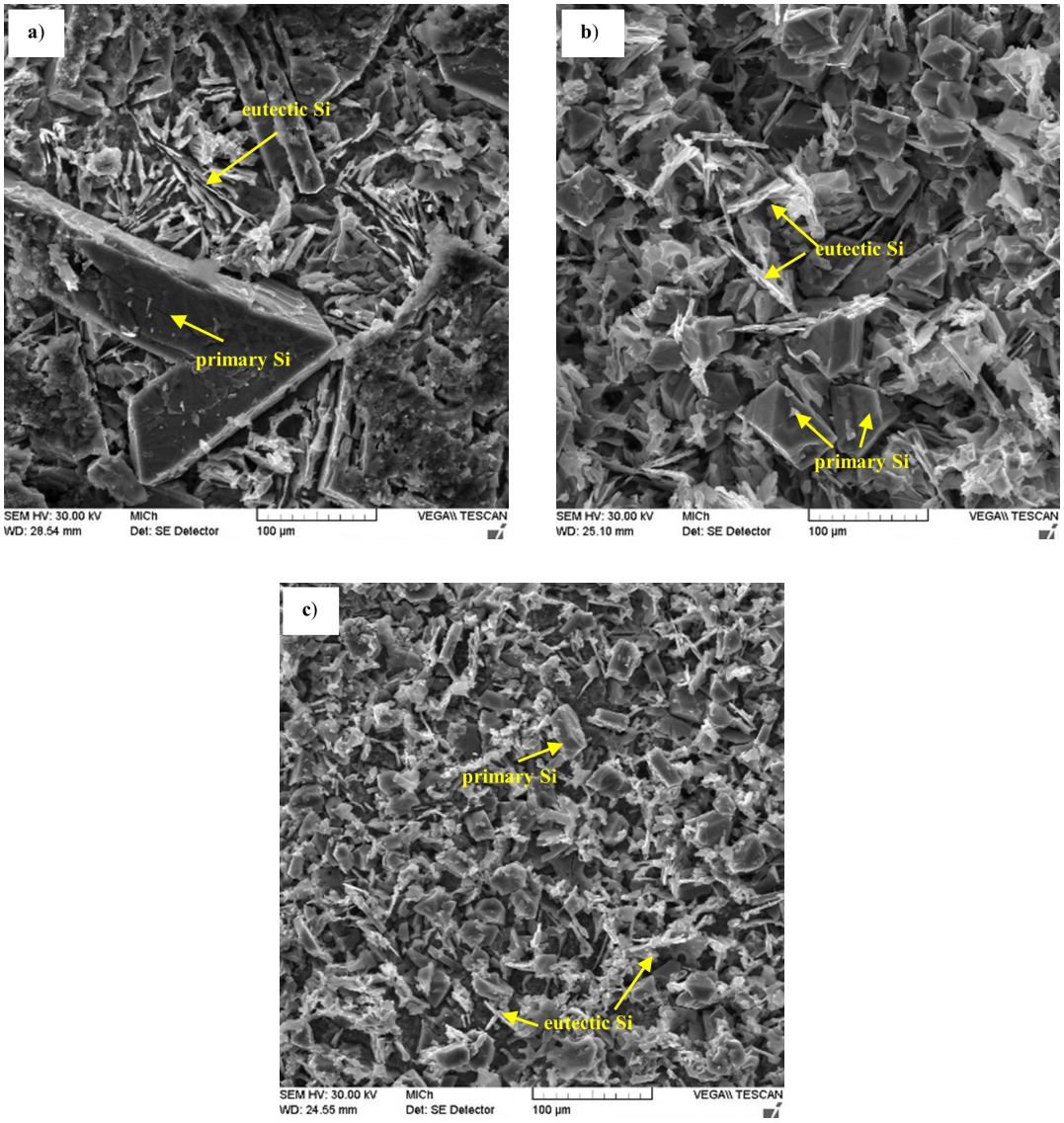

Fig. 4. Morphology of primary and eutectic silicon: a) alloy A, b) alloy B, c) alloy C; deep-etched by HCl, SEM

The morphology of eutectic Si after the deep etching in alloys without AlCu19P1.4 and with AlCu19P1.4 is documented by SEM in Figs. 2, 3 and 4. By comparing the microstructures in the unmodified alloy and the alloys after AlCu14P1.4 additions, it was found that the morphology of the eutectic Si remains unchanged and has a plate-like shape in all experimental alloys. This indicates that probably modification with this AlCu14P1.4 pre-alloy has no positive effect on nucleation and growth of eutectic Si. We did not observe a change in the shape of the eutectic silicon even after the addition of the Fe – micro additive, too.

4. CONCLUSIONS

The effective combination of AlCu14P1.4 pre-alloy and Fe-micro additive on the morphology of primary and eutectic Si in progressive AlSi21CuNiMg cast alloy was investigated.

From the experiments, the following results were obtained:

- Adding AlCu14P1.4 to the experimental alloys significantly reduces the size and increases the number of primary Si particles.
- Morphology of the primary Si changes from star-like, polyhedral, or plate-like in the alloy without the AlCu19P1.4 to finer polyhedral or plate-like after the addition of AlCu19P1.4 to the experimental alloy.
- The best refining and modification effect can be achieved when the AlCu14P1.4 with 0.02% Fe micro-additive is added to the melt.
- The addition of the AlCu14P1.4 pre-alloy has no effect on the morphology changes of the eutectic Si (this becomes plate-like).
- Deep etching with HCl proved to be suitable for observing the 3D morphology of primary or eutectic silicon on SEM. Although the depth etching is simple in principle, it is not without problems. In achieving the desired morphology of the phases in the structure under investigation, it is neces-

sary to ensure that the shape and surface of these etched phases are preserved without significant etching products and artefacts.

ACKNOWLEDGEMENTS

Recognition for financial support of the experimental work includes the Scientific Grand Agency of the Ministry of Education of the Slovak Republic and the Slovak Academy of Sciences (project VEGA 01/0398/19), the University of Žilina (support young researchers at UNIZA – ID project 12715) and the EÚ (project 313011ASY4 "Strategic implementation of additive technologies to strengthen the intervention capacities of emergencies caused by the COVID-19 pandemic").

REFERENCES

[1] J. Jorstad and D. Apelian, "Hypereutectic Al–Si Alloys: Practical Casting Considerations," *Int. J. Metalcast.*, vol. 3, pp. 13–36, 2009, doi: 10.1007/BF03355450.

[2] S. Meng, S. Wu, X. Wang, and L. Wan, "Effects of Co addition on Fe-bearing intermetallic compounds and mechanical properties of AlSi20Cu2Ni1Fe0.7-1 alloys," *J. Alloy. Compd.*, vol. 551, pp. 468–474, 2013, doi: 10.1016/j.jallcom.2012.10.181.

[3] C. Gong, H. Tu, C. Wu, J. Wang, and X. Su, "Study on Microstructure and Mechanical Properties of Hypereutectic Al-18Si Alloy Modified with Al-3B," *Materials*, vol. 11, pp. 456, 2018, doi: 10.3390/ma11030456.

[4] J. Pezda, "Assessment of AlSi21CuNi Alloy's Quality with Use of ATND Method," *Arch. Foundry Eng.*, vol. 13, no. 4, pp. 87–92, 2013, doi: 10.2478/afe-2013-0088.

[5] Z. Zhang, H-T. Li, I.C. Stone, and Z. Fan, "Refinement of primary Si in hypereutectic Al–Si alloys by intensive melt shearing," in *IOP Conf. Ser.: Mater. Sci. Eng.,* vol. 27, p. 012042, 2011, doi: 10.1088/1757-899X/27/1/012042.

[6] J. Wang, Z. Guo, J.L. Song, W.X. Hu, J.C. Li, and S.M. Xiong, "Morphology transition of the primary silicon particles in a hypereutectic A390 alloy in high pressure die casting," *Sci. Rep.*, vol. 7, p. 14994, 2017, doi: 10.1038/s41598-017-15223-w.

[7] Foundry Technologies & Engineering GmbH. [Online]. Available: https://www.giessereilexikon.com

[8] P. Jiandon and S. Talangkun, "Microstructural Modification Hardness and Surface Roughness of Hypereutectic Al–Si Alloys by A Combination of Bismuth and Phosphorus," *Crystals*, vol. 12, p. 1026, 2022, doi: 10.3390/cryst12081026.

[9] P. Xing, B. Gao, Y. Zhuang, K. Liu, and G. Tu, "On the modification of hypereutectic Al–Si alloys using rare earth Er," *Acta Metall. Sin.-Engl. Lett.*, vol. 23, no. 5, pp. 327–333, 2010, doi: 10.11890/1006-7191-105-327.

[10] L. Zhang, S. Chen, Q. Li, G. Chang, "Formation mechanism and conditions of fine primary silicon being uniformly distributed on single αAl matrix in Al–Si alloys," *Mater. Des.*, vol. 193, pp. 108853, 2020, doi: 10.1016/j.matdes.2020.108853.

[11] M. Michalski and F. Romankiewicz, "AlSi21CuNi silumin modification with phosphor and strontium micro additions", in *E3S Web Conf.,* vol. 19, p. 03026, 2017, doi: 10.1051/e3sconf/20171903026.

[12] E. Tillová, M. Farkašová, and M. Chalupová, "The role of antimony in modifying of Al–Si–Cu cast alloy," *Manuf. Technol.*, vol. 13, no. 1, pp. 109–114, 2013, doi: 10.21062/ujep/x.2013/a/1213-2489/MT/13/1/109.

[13] M. Farkašová, E. Tillová, and M. Chalupová, "Modification of Al–Si-Cu cast alloy," *FME Trans.*, vol. 41, no. 3, pp. 210–215, 2013.

[14] K. Borko, E. Tillová, and M. Chalupová, "The impact of Sr content on Fe – intermetallic phase's morphology changes in alloy AlSi10MgMn," *Manuf. Technol.*, vol. 16, no. 1, pp. 20–26, 2016, doi: 10.21062/ujep/x.2016/a/1213-2489/MT/16/1/20.

[15] Q. Li, B. Li, J. Li, Y. Zhu, and T. Xia, "Effect of yttrium addition on the microstructures and mechanical properties of hypereutectic Al-20Si alloy," *Mater. Sci. Eng. A*, vol. 722, 2018, pp. 47–57, doi: 10.1016/j.msea.2018.03.015.

[16] M. Zuo, X.F. Liu, Q.Q. Sun, and K. Jiang, "Effect of rapid solidification on the microstructure and refining performance of an Al–Si–P master alloy," *J. Mater. Process. Technol.*, vol. 209, no. 15–16, pp. 5504–5508, 2009, doi: 10.1016/j.jmatprotec.2009.05.005.

[17] W.M. Mao, P.Y. Yan, and Z.K. Zheng, "Refinement of primary silicon grains in semi-solid al-25% Si hypereutectic aluminium alloy slurry," *Solid State Phenomena*, vol. 285, pp. 153–160, 2019, doi: 10.4028/www.scientific.net/SSP.285.153.

[18] L. Dehong, J. Yehua, G. Guisheng, Z. Rongfeng, L. Zhenhua, and Z. Rong, "Refinement of primary Si in hypereutectic Al–Si alloy by electromagnetic stirring," *J. Mater. Process. Technol.*, vol. 189, no. 1–3, pp. 13–18, 2007, doi: 10.1016/j.jmatprotec.2006.12.008.

[19] Q.C. Zou, J.C. Jie, J.L. Sun, T.M. Wang, Z.Q. Cao, and T.J. Li, "Effect of Si content on separation and purification of the primary Si phase from hypereutectic Al–Si alloy using rotating magnetic field," *Sep. Purif. Technol.*, vol. 142, pp. 101–107, 2015, doi: 10.1016/j.seppur.2015.01.005.

[20] X. Bian and W. Wang, "Thermal-rate treatment and structure transformation of Al-13wt.% Si alloy melt," *Mater. Lett.*, vol. 44, no. 1, pp. 54–58, 2000, doi: 10.1016/S0167-577X(00)00011-2.

[21] A.V. Pozdniakov, M.V. Glavatskikh, S.V. Makhov, and V.I. Napalkov, "The synthesis of novel powder master alloys for the modification of primary and eutectic silicon crystals," *Mater. Lett.*, vol. 128, pp. 325–328, 2014, doi: 10.1016/j.matlet.2014.04.068.

[22] Z. Min and L. Xiangfa, "Series of Al–P Master Alloy and excellent refining performance on hypereutectic A390 Alloys," *Adv. Mater. Res.,* vol. 306–307, pp. 613–616, 2011, doi: 10.4028/www.scientific.net/AMR.306-307.613.

[23] J. Piątkowski, "The phosphorus interaction on the process forming of primary structure of hypereutectic silumins," *Arch. Foundry Eng.*, vol. 9, no. 3, pp. 125–128, 2009.

[24] M. Zuo, D. Zhao, X. Teng, H. Geng, and Z. Zhang, "Effect of P and Sr complex modification on Si phase in hypereutectic Al-30Si alloys," *Mater. Des.*, 47, pp. 857–864, 2013, doi: 10.1016/j.matdes.2012.12.054.

[25] B. Heshmatpour, "Modification of Silicon in Eutectic and Hyper-Eutectic Al–Si Alloys", in *Essential Readings in Light Metals.* J.F. Grandfield, D.G. Eskin, Eds., Springer, Cham, 2016, doi: 10.1007/978-3-319-48228-6_53.

[26] R. Romankiewicz and F. Romankiewicz, "Influence of modification on the refinement of primary silicon crystals in hypereutectic silumin AlSi21CuNi," *Prod. Eng. Arch.*, vol. 19, pp. 30–36, 2018, doi: 10.30657/pea.2018.19.07.

[27] T. Lipinski, "Modification of AlSi21CuNi alloy by fast cooled alloy with Al, B and Ti", in *Proceedings of the international scientific conference Engineering for Rural Development*, Latvia, 2016, pp. 940–945.

[28] B. Bryksí Stunová and D. Henzl, "Aluminium alloys for combustion engines and compressors pistons," *Slévárenství*, vol. LXIV, no. 3–4, pp. 82–85, 2016.

[29] L. Kuchariková, E. Tillová, M. Bonek,, and M. Chalupová, "Using deep etching in the study of eutectic silicon 3D-morphology in AlSi7MgTi cast alloy," *Arch. Metall. Mater.*, vol. 63, no. 4, pp. 2017–2022, 2018, doi: 10.24425/amm.2018.125138.

[30] L. Kuchariková, E. Tillová, J. Belan, A. Vaško, and I. Švecová, "Quantitative assessment of aluminium cast alloys´structural parameters to optimize its properties," *Metalurgija*, vol. 56, no. 1–2, pp. 145–148, 2017. [Online]. Available: https://hrcak.srce.hr/168914 [Accessed 22.08.2022].

[31] V. Vijeesh and P.K. Narayan, "Review of Microstructure Evolution in Hypereutectic Al–Si Alloys and its Effect on Wear Properties," *Trans. Indian Inst. Met.*, vol. 67, pp. 1–18, 2014, doi: 10.1007/s12666-013-0327-x.

[32] C.L. Xu, H.Y. Wang, C. Liu, and Q.C. Jiang, "Growth of octahedral primary silicon in cast hypereutectic Al–Si alloys," *J. Cryst. Growth*, vol. 291, pp. 540–547, 2006, doi: 10.1016/j.jcrysgro.2006.03.044.

[33] M.M. Makhlouf and H.V. Guthy, "The aluminum-silicon eutectic reaction: mechanisms and crystallography," *J. Light Met.*, vol. 1, no. 4, pp. 199–218, 2001, doi: 10.1016/S1471-5317(02)00003-2.

[34] D.R. Hamilton and R.G. Seidensticker, "Growth Mechanisms of Germanium Dendrites: Kinetics and the Nonisothermal Interface," *J. Appl. Phys.*, vol. 34, no. 5, pp. 1450–1460, 1963, doi: 10.1063/1.1729599.

[35] F. Mao *et al.*, "Different Influences of Rare Earth Eu Addition on Primary Si Refinement in Hypereutectic Al–Si Alloys with Varied Purity," *Materials*, vol. 12, p. 3505, 2019, doi: 10.3390/ma12213505.